

The β C–C bond scission in alkoxy radicals: thermal unimolecular decomposition of *t*-butoxy radicals

Christa Fittschen,^a Horst Hippler^{*b} and Béla Viskolcz^b

^a Laboratoire de Cinétique et Chimie de la Combustion—UMR 8522, Centre d'Etudes et de Recherches Lasers et Applications Université de Lille 1, F-59655 Villeneuve d'Ascq Cedex, France

^b Lehrstuhl für Molekulare Physikalische Chemie, Universität Karlsruhe, Kaiserstrasse 12, D-76128 Karlsruhe, Germany. E-mail: horst.hippler@chemie.uni-karlsruhe.de; Fax: +49 721 608 6524; Tel: +49 721 608 3301

Received 4th January 2000, Accepted 11th February 2000

The temperature and pressure dependence of the unimolecular decomposition of *t*-butoxy radicals was studied by the laser photolysis/laser induced fluorescence technique. Experiments have been performed at total pressures between 0.04 and 60 bar of helium and in the temperature range 323–383 K. The low and the high pressure limiting rate constants as well as the broadening factor F_c have been extracted from a complete falloff analysis of the experimental results: $k_0 = [\text{He}] \times 1.5 \times 10^{-8} \exp(-38.5 \text{ kJ mol}^{-1}/RT) \text{ cm}^3 \text{ s}^{-1}$, $k_\infty = 1.0 \times 10^{14} \exp(-60.5 \text{ kJ mol}^{-1}/RT) \text{ s}^{-1}$, and $F_c = 0.87 - T/870 \text{ K}$. We anticipate an uncertainty for these rate constants of $\pm 30\%$. Important features of the potential energy surface have been computed by *ab initio* methods. The Arrhenius parameters for the high pressure limiting rate constant for the β C–C bond scission of *t*-butoxy radicals have been computed from the properties of a transition state based on the results of G2(MP2) *ab initio* calculation. The results from density functional theory (DFT) with a small basis set (B3LYP/SVP) are very similar. Excellent agreement between the calculated and the experimental rate constants has been found. We suggest a common pre-exponential factor for β C–C bond scission rate constants of all alkoxy radicals of $A = 10^{14 \pm 0.3} \text{ s}^{-1}$. Thus we express the high pressure limiting rate constant for ethoxy and *i*-propoxy radicals by $k_\infty = 1.0 \times 10^{14} \exp(-78.2 \text{ kJ mol}^{-1}/RT)$ and $1.0 \times 10^{14} \exp(-63.1 \text{ kJ mol}^{-1}/RT) \text{ s}^{-1}$, respectively. For the reverse reactions, the addition of CH_3 radicals to CH_2O , CH_3CHO , and $(\text{CH}_3)_2\text{CO}$, we obtained activation enthalpies of 32, 42, and 52 kJ mol^{-1} , respectively.

Introduction

In the photo-oxidation of saturated hydrocarbons in the atmosphere alkoxy radicals are important intermediates from NO oxidation to NO_2 . Low temperature combustion as well as pyrolysis of oxygen containing compounds proceed *via* alkoxy radicals. Therefore, many experimental studies have been devoted to alkoxy radical reactions and several review articles have appeared.^{1–5} Earlier data on the decomposition of alkoxy radicals are mainly based on the work of Batt² and were focused on atmospheric pressure conditions.^{6,7}

Recently, new experimental^{8–11} and theoretical^{12–14} studies have been carried out on the unimolecular reactions of alkoxy radicals. It was found that for ethoxy, *i*-propoxy and *t*-butoxy the β C–C bond dissociation dominates over all other intramolecular processes. For ethoxy¹¹ and *i*-propoxy,⁹ the falloff is centered near 1 bar and the studied pressure range extends over several orders of magnitude in pressure up to 60 bar. Also for the *t*-butoxy radical decomposition a pressure dependence has been reported^{15–18} and recently⁸ it was found that the falloff was centered near 200 mbar. However, since *t*-butoxy is a relatively large radical we expected a broad falloff range and the pressure dependence to continue above atmospheric pressure.

This study on the thermal decomposition of *t*-butoxy radicals completes the different cases for β C–C bond dissociation of alkoxy radicals. In *t*-butoxy the radical center at the oxygen atom is connected to a tertiary carbon atom while in ethoxy¹¹

and *i*-propoxy⁹ the radical center is connected to a primary and secondary carbon atom, respectively. The *t*-butoxy radical is a prototype for the β C–C bond dissociation of larger alkoxy radicals since β C–H bond dissociation does not exist and 1,3-hydrogen transfer isomerizations are energetically disfavored because of the high strain energy of the cyclic transition state resulting in a threshold energy about 40 kJ mol^{-1} higher than for the β C–C bond dissociation.



The *ab initio* study of the potential energy surface for two different decomposition channels enabled us to theoretically analyze the falloff curves and also to predict the high pressure limiting rate constant from a RRKM calculation using a simple transition state model (TST).

In the present work we have investigated the decomposition of *t*-butoxy radicals at different temperatures over several orders of magnitude in pressure. Our intention was to experimentally access most of the falloff range which will then allow for a reliable determination of the limiting high and low pressure rate constants. We combined our experiments with *ab initio* calculations and identified the unimolecular β C–C bond scission as the dominant decomposition channel. The experimental high pressure limiting rate constant will be compared to the result from a simple RRKM calculation using the *ab initio* transition state. The analysis of the low pressure limiting rate constant should deliver valuable information on the collisional energy transfer. Based on our present and earlier

experimental results on the β C–C bond scission of alkoxy radicals, we predict Arrhenius parameters for β C–C bond cleavage of many other alkoxy radicals and also for the corresponding reverse reaction.

Experimental

Experiments have been performed by laser flash photolysis (LFP) of *t*-butylnitrite (*t*-C₄H₉ONO) under high helium pressures (0.04–60 bar) and *t*-butoxy radicals were detected by laser induced fluorescence. Details of the experimental set-up have been described recently^{9,11} so only some principal features are given here:

Like all alkyl nitrites, *t*-butylnitrite has two absorption bands in the UV region particularly suitable for excimer laser photolysis: one broad band with a maximum at 223 nm and a decadic absorption coefficient of $\epsilon(223 \text{ nm}) = 1750 \text{ l mol}^{-1} \text{ cm}^{-1}$ and a second weaker and more structured transition near 360 nm [$\epsilon(353.6 \text{ nm}) = 37 \text{ l mol}^{-1} \text{ cm}^{-1}$].¹⁹ The *t*-butylnitrite has mostly been photolysed at 351 nm and only few experiments with 248 nm photolysis have been performed. However, at low pressures thermalization of the *t*-butoxy radicals from 248 nm photolysis could not be achieved.

The photolysis laser beam (Lambda Physik LPX 202i) was focused with two cylindrical lenses, leading to average pulse energies of 50 mJ cm^{-2} at 351 nm. The *t*-C₄H₉ONO concentrations have been varied up to $5 \times 10^{15} \text{ cm}^{-3}$. With a decadic absorption coefficient of $\epsilon(351 \text{ nm}) = 27 \text{ l mol}^{-1} \text{ cm}^{-1}$ ¹⁹ and an assumed photodissociation quantum yield of unity the *t*-C₄H₉O[•] radical concentration was always below $4.5 \times 10^{13} \text{ cm}^{-3}$.

We followed the temporal evolution of the *t*-C₄H₉O[•] radical concentration by laser induced fluorescence (LIF), excited near 335 nm. The fluorescence was collected perpendicular to the fluorescence excitation laser beam through a cut-off filter at $\lambda > 375 \text{ nm}$. The room temperature fluorescence excitation spectrum has been normalized with respect to the energy of the excitation laser pulse and is displayed in Fig. 1. As expected, the structure in our spectrum is much more congested compared to the low temperature spectra at 203 K from Blitz *et al.*⁸ and at 213 K from Wang *et al.*²⁰ The fluorescence lifetime τ_{fl} is given by the following expression:

$$\tau_{\text{fl}}^{-1} = \tau_{\text{rad}}^{-1} + k_{\text{q}}[t\text{-C}_4\text{H}_9\text{ONO}] + k_{\text{q, He}}[\text{He}] \quad (2)$$

in which τ_{rad} is the radiative lifetime and k_{q} and $k_{\text{q, He}}$ are the fluorescence quenching rate constant with the precursor *t*-butylnitrite and with He, respectively. Quenching by *t*-butylnitrite was very efficient and from the shortening of the fluorescence lifetime (see Fig. 2) we found a rate constant of $k_{\text{q}} = (4.3 \pm 0.2) \times 10^{-10} \text{ cm}^3 \text{ s}^{-1}$. The radiative lifetime was

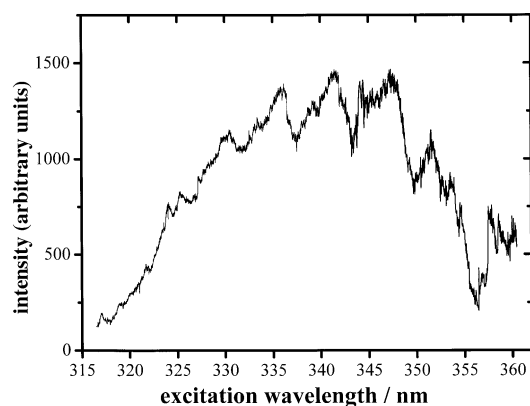


Fig. 1 Fluorescence excitation spectrum of *t*-butoxy radicals at 298 K.

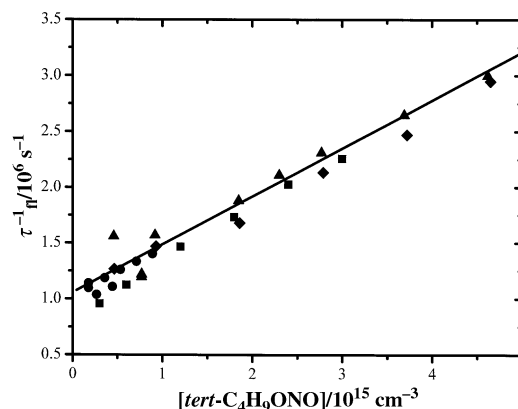


Fig. 2 Fluorescence lifetime τ_{fl} of *t*-butoxy radicals excited at 335 nm as a function of the precursor concentration ($T = 323 \text{ K}$; ●: $p(\text{He}) = 26 \text{ Torr}$; ▲: $p(\text{He}) = 100 \text{ Torr}$; ■: $p(\text{He}) = 316 \text{ Torr}$; ◆: $p(\text{He}) = 737 \text{ Torr}$).

found to be $\tau_{\text{rad}} = (1.0 \pm 0.1) \times 10^{-6} \text{ s}$. As seen in Fig. 2 quenching is more or less independent on helium addition between 26 and 737 Torr and we estimate an upper limit of the quenching rate constant at room temperature of $k_{\text{q, He}} < 5 \times 10^{-15} \text{ cm}^3 \text{ s}^{-1}$. Our radiative lifetime is much longer than previously reported lifetimes of 500 ns by Blitz *et al.*⁸ and of 150 ns by Wang *et al.*²⁰ The shorter lifetimes might result from the efficient quenching by the parent molecules or from uncompleted thermalization of the *t*-butoxy radicals when the excitation laser has been fired.

The *t*-butylnitrite (Aldrich, 96%) was used without further purification after extensive degassing in various freeze pump cycles. Gaseous mixtures, highly diluted in He, did not markedly decompose at room temperature in a darkened glass bulb or stainless steel cylinder. The carrier gas He (99.995%, Air Liquide) was used without further purification.

The helium pressure in the experiments extended from 0.04 to 60 bar and the temperature range was restrained between 323 and 383 K. At the high temperature limit *t*-butoxy radical decomposition approached the time resolution of the experiments while below the low temperature limit unimolecular decomposition could no longer be separated from *t*-butoxy loss in bimolecular reactions.

Theoretical methods

Different theoretical methods were tested in two recent papers to obtain reliable potential energy surfaces for β C–C bond dissociation of ethoxy¹¹ and *i*-propoxy radicals.⁹ Consequently, we selected the modified G2(MP2) method for the *t*-butoxy decomposition, expecting the most accurate results. All *ab initio* calculations were carried out using the GAUSSIAN 94 program package.²¹

The equilibrium geometries, transition structures, and harmonic vibrational frequencies were obtained on the MP2/6-311G** level. The height of the barriers were calculated from the classical barrier heights (obtained as the *ab initio* energy differences) by adding the difference of the vibrational zero-point energies scaled by the factor of 0.9748 as recommended by Scott and Radom²². Activation enthalpies were obtained by adding the thermal contributions. The standard enthalpy of reaction at 298.15 K was taken as the enthalpy difference between the products and the *t*-butoxy radical.

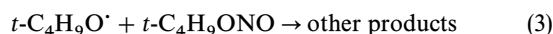
For comparison we also performed DFT calculations as undertaken before for the ethoxy radical.¹¹ We found again that extended basis sets definitely underestimate the barrier heights and reaction enthalpies and that the predicted transition state structures are relatively loose. These loose transition states will lead to an overestimation of the preexponential factor of the high pressure limiting dissociation

rate constant. However, very good agreement with energies from the expensive G2(MP2) method has been obtained using the much cheaper B3LYP hybrid functional²³ combined with the SVP basis set from Ahlrichs and co-workers.²⁴

Results

Experimental results

Under our experimental conditions *t*-butoxy radicals decay predominantly by unimolecular decomposition in reaction (1) and to a lesser extent by a bimolecular reaction with the precursor



Accordingly, the *t*-butoxy radical decay follows a pseudo-first-order rate law

$$\frac{d[t\text{-C}_4\text{H}_9\text{O}^\bullet]}{dt} = -k_{\text{obs}}[t\text{-C}_4\text{H}_9\text{O}^\bullet] \quad (4)$$

where the total pseudo-first-order rate constant k_{obs} is given by

$$k_{\text{obs}} = k_1 + k_3[t\text{-C}_4\text{H}_9\text{ONO}]. \quad (5)$$

Total pseudo-first order rate constants k_{obs} for the *t*-butoxy radical decay were obtained from plots of the fluorescence yields *vs.* the delay time between the two laser pulses. Typical decay curves of the *t*-C₄H₉O[•] fluorescence yield at 323 K and different total pressures are shown in Fig. 3.

The influence of reaction (3) on the total pseudo-first-order rate constant has carefully been investigated by running experiments with different precursor concentrations at all pressures and temperatures. The pseudo-first-order unimolecular decomposition rate constant k_1 has been obtained by an extrapolation of k_{obs} to a zero precursor concentration. An example of this procedure at 323 K and different total pressures is shown in Fig. 4. We obtained for the rate constant $k_3 = (5 \pm 2) \times 10^{-12} \text{ cm}^3 \text{ s}^{-1}$, temperature independent between 323 and 383 K. The extrapolation of k_{obs} was always straightforward but at low temperatures the relative contribution of reaction (3) to k_{obs} was generally larger than at high temperatures. The experimental conditions and the results of this procedure are represented in the supplementary Table S1.† The individual falloff curves for the first-order decomposition rate constant k_1 are illustrated in Fig. 5.

Ab initio calculations

There is a large variety of possible decomposition channels of the *t*-butoxy radical. The two energetically lowest channels are

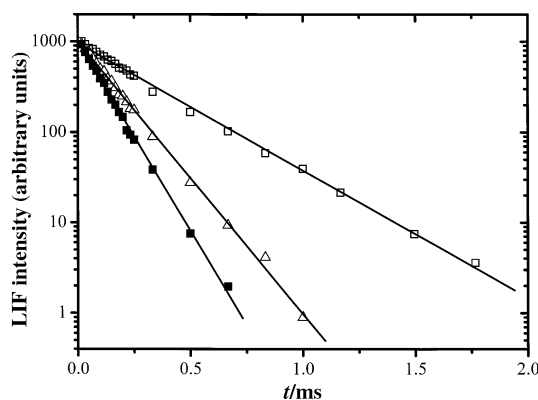


Fig. 3 Decay of *t*-butoxy fluorescence yields at different helium pressures [$T = 323 \text{ K}$; \square : 30 Torr; \triangle : = 219 Torr; \blacksquare : = 750 Torr; solid lines: best fit according to eqn. (4)].

† Available as electronic supplementary information. See <http://www.rsc.org/suppdata/cp/b0/b000009o>

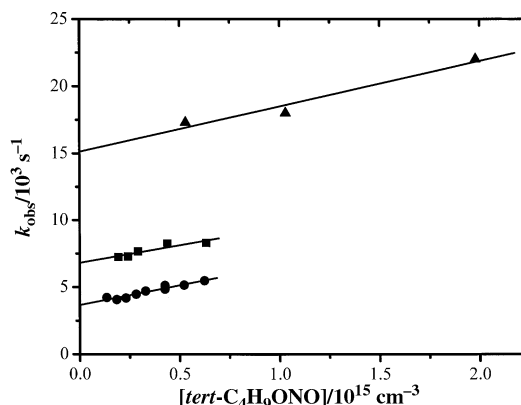


Fig. 4 Pseudo-first-order rate constant k_{obs} as a function of precursor concentrations ($T = 323 \text{ K}$; \blacktriangle : $p(\text{He}) = 7500 \text{ Torr}$; \blacksquare : $p(\text{He}) = 200 \text{ Torr}$; \bullet : $p(\text{He}) = 30 \text{ Torr}$).

the β C–C bond scission and the 1,3 hydrogen atom shift. It has been shown that the 1,3 isomerization transition states for the ethoxy¹⁰ and the *n*-butoxy radical¹³ contain high strain energies. We conclude, that for the *t*-butoxy radical the situation is similar and that under our conditions only the β C–C bond scission has to be considered.

The calculated MP2/6-311G(d,p) optimized geometries of the *t*-butoxy radical and the transition state (TS) are shown in Fig. 6. At the transition state the length of the breaking C–C bond has increased by about 30%, with respect to its lengths in the parent radical while the length of the C–O bond has already shortened and approaches the characteristic length of the C–O double bond. All other bond lengths remain almost unchanged during the reaction. The transition state structure is very much product-like as found previously for the β C–C

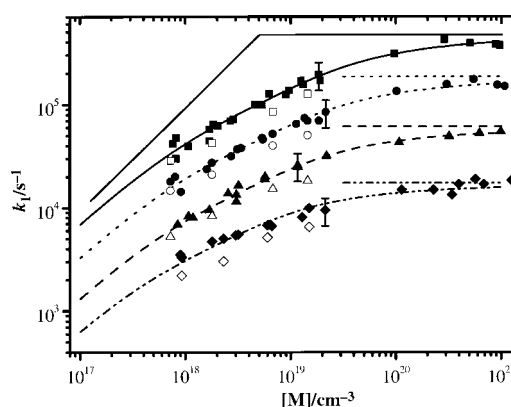


Fig. 5 Falloff curves of the first-order rate constants k_1 at different temperatures (\blacksquare and \square : $T = 383 \text{ K}$; \bullet and \circ : $T = 363 \text{ K}$; \blacktriangle and \triangle : $T = 343 \text{ K}$; \blacklozenge and \diamond : $T = 323 \text{ K}$; lines: best fit by eqn. (6) using the falloff parameters from Table 2; full symbols: this work; open symbols: ref. 8).

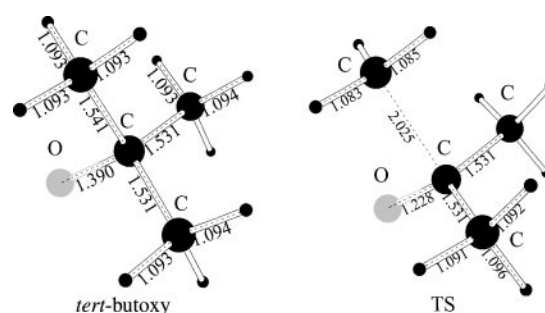


Fig. 6 Equilibrium geometry of the *t*-butoxy radical and structure of the transition state for the decomposition channel (1) optimized by MP2/6-311G**.

bond scission in ethoxy¹¹ and in i-propoxy.⁹ The TS geometry from the B3LYP/SVP method is somewhat more product-like than from the optimized MP2/6-311G(d,p) calculation.

The reaction barriers (E_0), activation enthalpies [$\Delta H^{0\ddagger}$ (298 K)], and activation entropies [$\Delta S^{0\ddagger}$ (298 K)] obtained at various levels of theory are presented in Table 1. There are significant differences in the barriers heights from various levels of theory. The lowest barrier of β C–C bond scission was always predicted by DFT with the extended basis set. However, the barrier predicted by B3LYP with smaller basis sets is in very good agreement with the higher level G2(MP2) barrier. The agreement between the barriers for the reverse reaction from the various methods was not very good. The reasons can be found in the reaction enthalpies which are correctly predicted to be positive by QCISD(T) and G2(MP2) and incorrectly predicted to be negative by the DFT and MP2 methods. The activation entropies [$\Delta S^{0\ddagger}$ (298 K)] using the different TS geometries and the scaled vibrational frequencies were always about $3 \text{ J mol}^{-1} \text{ K}^{-1}$ higher from the DFT calculation than from the MP2/6-311G** method.

The *ab initio* reaction enthalpies are also listed in Table 1. From standard reference data bases the reaction enthalpy $\Delta_{\text{R}}H^{\circ}$ (298 K) = 19.2 kJ mol^{-1} is obtained, using $\Delta_{\text{f}}H^{\circ}$ (CH_3 , 298 K) = 145.5 ,^{25,26} $\Delta_{\text{f}}H^{\circ}$ (*t*-C₄H₉O, 298 K) = -90.8 ,²⁷ and $\Delta_{\text{f}}H^{\circ}$ (acetone, 298 K) = $-217.1 \text{ kJ mol}^{-1}$,²⁸ respectively. From our G2(MP2) calculation we obtain a reaction enthalpy of $\Delta_{\text{R}}H^{\circ}$ (298 K) $\approx 7.4 \text{ kJ mol}^{-1}$ which is about 12 kJ mol^{-1} lower. For comparison, we computed the standard enthalpy of formation of *t*-C₄H₉O radicals by the modified G2(MP2) method combined with the tabulated heat of formation of the atoms. We obtained $\Delta_{\text{f}}H^{\circ}$ (*t*-C₄H₉O, 298 K) = $-81.3 \text{ kJ mol}^{-1}$ about 10 kJ mol^{-1} higher than the recommended value in ref. 27. For comparison, similarly 10 kJ mol^{-1} higher heats of formation of ethoxy¹¹ and i-propoxy⁹ radicals than currently accepted have recently been found. These higher values are in close agreement with results from *ab initio* calculations of the heats of formation of alkoxy radicals within the Gaussian-n²⁹ series.

Discussion

The falloff analysis of the *t*-butoxy decomposition rate constant is straightforward since we know from our *ab initio* treatment that the β C–C bond scission is the energetically distinctly favored pathway. We therefore describe the experimentally obtained falloff curves by the expression developed

by Troe *et al.*^{30,31}

$$\log\left(\frac{k_1}{k_{1,\infty}}\right) = \log\left(\frac{k_{1,0}/k_{1,\infty}}{1 + k_{1,0}/k_{1,\infty}}\right) + \frac{\log F_c}{1 + (\log(k_{1,0}/k_{1,\infty}))/N)^2} \quad (6)$$

In this expression the parameters $k_{1,0}$, $k_{1,\infty}$ and F_c are respectively the low pressure rate constant, the high pressure rate constant and the broadening factor. The procedure of the analysis of the experimental results has been described in detail in previous publications.^{9,11}

The experimental results allow for a reliable determination of the high pressure limiting rate constants (see Fig. 5) which are also given in Table 2. We represent these rate constants in an Arrhenius expression and account for an uncertainty in the rate constant of $\pm 30\%$ comprehending essentially the reliability of the fall off extrapolation:

$$k_{1,\infty} = 1.0 \times 10^{14} \exp(-60.5 \text{ kJ mol}^{-1}/RT) \text{ s}^{-1} \quad (323 \text{ K} < T < 383 \text{ K}) \quad (7)$$

Our high pressure Arrhenius parameters are slightly different from the values given by Blitz *et al.*⁸ Presumably this difference has its source in the smaller range of pressure covered by Blitz *et al.* It should be pointed out that the experimental accessible temperature range is much too small to reliably separate the *A*-factor from the activation energy. We therefore fixed the *A*-factor to $A = 1.0 \times 10^{14} \text{ s}^{-1}$ in agreement with the transition state model from the *ab initio* calculations (see below). Although the absolute rate constants of the two studies agree reasonably well, it should be pointed out that our dissociation rate constants are moderately and systematically higher than the values from Blitz *et al.*⁸ (see Fig. 5). The reason for this difference is yet unknown and may be due to slightly different temperatures in the two experiments. It is very well known that fast gas flows into thermalized reactors do not instantaneously thermally equilibrate. To check this we have varied the flow rate at constant pressure and carefully determined the rate of unimolecular decomposition as previously undertaken for the i-propoxy radical.⁹ At low flow rates we found a constant flow independent *t*-butoxy decomposition rate which considerably decreased with increasing the flow rate thus reflecting incomplete heating of the gas flow. We conclude that the systematic difference in the two experimental results is in conformity with a temperature difference of about 3 K in the two experimental arrangements.

Table 1 Activation barriers E_0 , activation enthalpies $\Delta H^{0\ddagger}$ (298 K), activation entropies $\Delta S^{0\ddagger}$ (298 K) and standard reaction enthalpies $\Delta_{\text{R}}H^{\circ}$ (298 K) of the C–C bond dissociation as well as the high pressure limiting rate constant (energies and enthalpies in kJ mol^{-1} ; entropies in $\text{J K}^{-1} \text{ mol}^{-1}$)

Method	E_0	$\Delta H^{0\ddagger}$ (298 K)	$\Delta S^{0\ddagger}$ (298 K)	$\Delta_{\text{R}}H^{\circ}$ (298 K)	$k_{\infty}/10^3 \text{ s}^{-1}$ ($T = 323 \text{ K}$)
B3LYP/SVP	56.7	58.3	14.0		14
B3LYP/6-311 + G(3df,2p) ^a	49.4	50.5	11.0	-9.6	170
MP2/6-311G(d,p) ^a	79.6	80.8	11.0	-1.8	0.002
MP2/6-311 + G(3df,2p) ^a	67.5	68.7	11.0	-8.5	0.2
QCISD(T)/6-311G(d,p) ^a	69.8	70.9	11.0	14.1	0.09
G2(MP2)-like ^a	57.6	58.8	11.0	7.4	7.8
Experiment (ref. 7)		54.5			8.4
This work		58.0			18

^a MP2/6-311G(d,p) geometries and frequencies.

Table 2 Falloff parameters for the thermal decomposition of the *t*-butoxy radical for different temperatures

T/K	$(k_{1,0}/[\text{He}])/10^{-14} \text{ cm}^3 \text{ s}^{-1}$	$k_{1,\infty}/10^4 \text{ s}^{-1}$	F_c	β_c	$-\langle\Delta E\rangle_{\text{all}}/\text{cm}^{-1}$
323	0.90	1.75	0.50	0.050	21
343	1.78	6.14	0.47	0.040	18
363	4.41	18.8	0.45	0.0345	17
383	9.32	48.4	0.43	0.031	16

The high pressure limiting rate constant has almost been reached at the highest pressures of 60 bar helium. We analyzed this rate constant in terms of a simple transition state theory analysis.

$$k_{\text{th}, \infty} = \frac{k_{\text{B}}T}{h} \times \exp\left(\frac{\Delta S^{\ddagger 0}}{R}\right) \times \exp\left(-\frac{\Delta H^{\ddagger 0}}{RT}\right) \quad (8)$$

Using the parameters of Table 1 we calculate on the G2(MP2) level at 323 K high pressure limiting rate constants of $k_{\text{th}, \infty} = 7.8 \times 10^3 \text{ s}^{-1}$ in excellent agreement with the experimental value of $k_{1, \infty} = 1.7 \times 10^4 \text{ s}^{-1}$ from eqn. (7). From the B3LYP/SVP method which is computationally much cheaper we obtain $k_{\text{th}, \infty} = 1.4 \times 10^4 \text{ s}^{-1}$ also in excellent agreement with the experiment. However, B3LYP with larger basis sets overestimates the high pressure rate constant by about a factor of 10. A comparison of experimental and theoretically predicted high pressure limiting rate constants for the β C–C bond scission of *t*-butoxy is represented in Fig. 7. For the β C–C bond scission of small alkoxy radicals the reliability of the results from the cheap DFT small basis set calculations has been demonstrated. We conclude that this method can be used to predict rate constants for the β C–C bond scission of larger alkoxy radicals which are difficult to measure and very expensive to calculate with a high level *ab initio* method.

The strong collision low pressure limiting rate constant was calculated using the formalism proposed by Troe³² by taking the molecular parameters from the *ab initio* calculations as given in the Appendix. The density of states was calculated with the Whitten–Rabinovitch approximation³³ and the correction factors F_{E} and F_{anh} were determined as described in refs. 30 and 31. We did not explicitly take into account internal rotations but used the maximum F_{rot} . The collision efficiency β_{c} was obtained from a comparison with the low pressure limiting rate constant extrapolated from the experimental data. Since the collision efficiency effects the total broadening factor F_{C} we repeated this procedure until a theoretically consistent falloff curve was obtained. The final individual falloff curves are shown in Fig. 5 together with the experimental results. The falloff parameters are given in Table 2. We expressed the low pressure limiting rate constant as:

$$k_{1,0} = [\text{He}] \times 1.5 \times 10^{-8} \exp(-38.5 \text{ kJ mol}^{-1}/RT) \text{ cm}^3 \text{ s}^{-1} \quad (323 \text{ K} < T < 383 \text{ K}) \quad (9)$$

Taking into account the experimental uncertainties and the fact that falloff effects do influence the extrapolation of the low pressure rate constant, we estimate an uncertainty of this rate constant of 30%. It should be pointed out, that the limited

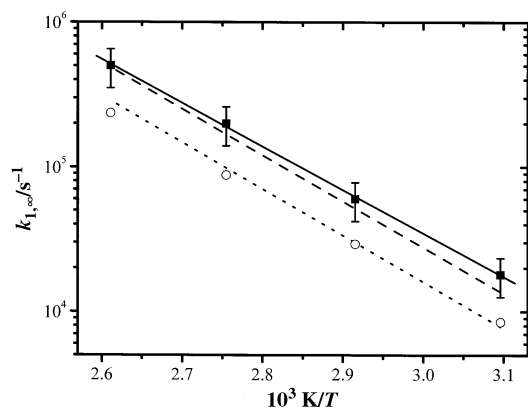


Fig. 7 Experimental and theoretical high pressure limiting rate constant for reaction (1) (○: from ref. 8; ■: this work; solid line: high pressure limit as given in eqn. (7); dotted line: TST-calculation based on the G2MP2; dashed line: TST-calculation based on the B3LYP/SVP).

temperature range of our experiments does not allow for a good separation of the pre-exponential factor from the activation energy of eqn. (9). The agreement with the recently published extrapolated low pressure expression⁸ is satisfactory although our *A*-factor is about 10 times higher, which is mostly compensated by our 6 kJ mol⁻¹ higher activation energy. In Fig. 8 we compare the strong collision as well as the weak collision low pressure rate constants as a function of temperature.

From our falloff analysis we extracted the broadening factor F_{C} and the collision efficiencies β_{c} between 323 and 383 K, respectively (see Table 2). Within the temperature range of our experiments the slightly negative temperature dependence of the broadening factor F_{C} is expressed as:

$$F_{\text{C}} = 0.87 - T/870 \text{ K} \quad (323 \text{ K} < T < 383 \text{ K}) \quad (10)$$

According to the expression³¹

$$\frac{\beta_{\text{c}}}{1 - \sqrt{\beta_{\text{c}}}} = \frac{-\langle \Delta E \rangle}{F_{\text{E}} kT} \quad (11)$$

very low average energies transferred per collision with helium of $\langle \Delta E \rangle = 21$ and -16 cm^{-1} at 323 and 383 K, respectively, are found (see Table 2). One might state that the $-\langle \Delta E \rangle$ values are low, however, they are in perfect agreement with the almost temperature independent $\langle \Delta E \rangle$ values of about -22 and -24 cm^{-1} for *i*-propoxy and ethoxy radicals in helium.^{9,11}

Implications for β C–C bond scission of alkoxy radicals

The excellent agreement between the experimental high pressure limiting rate constant and the theoretical result from a simple transition state treatment (TST) based on *ab initio* methods is very satisfactory. In particular, as the transition state properties from expensive G2 and G2(MP2) *ab initio* calculations are very similar to the energy and structure of the transition state from cheap small basis set DFT (B3LYP/SVP) calculations. The agreement between the results from high level *ab initio* treatments and small basis set DFT calculations holds for the three classes of alkoxy radicals, in which the radical center is connected to a primary (ethoxy),¹¹ secondary (*i*-propoxy)⁹ and tertiary (*t*-butoxy) carbon atom, respectively. For *t*-butoxy decomposition the experimental and theoretically predicted high pressure limiting rate constants agree within the experimental uncertainty of about $\pm 30\%$. A comparison is given in Fig. 7. We have shown, that for the three classes of β C–C bond scission of alkoxy radicals cheap small basis set DFT calculations provide reliable transition state structures and energies. On this evidence we calculated the

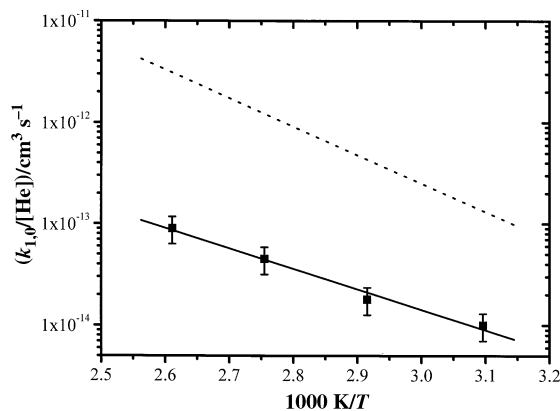


Fig. 8 Strong and weak collision second-order low pressure limiting rate constants $k_{1,0}/[\text{He}]$ (■: this work; solid line: weak collision rate constant as given by eqn. (9); dashed line: calculated strong collision rate constant).

Table 3 Activation barriers E_0 , activation enthalpies $\Delta H^{0\ddagger}$ (298 K), activation entropies $\Delta S^{0\ddagger}$ (298 K), and high pressure Arrhenius preexponential factor of the C–C bond dissociation as well as the Arrhenius activation energy from B3LYP/SVP calculations (energies and enthalpies in kJ mol^{-1} ; entropies in $\text{J K}^{-1} \text{mol}^{-1}$)

Reaction	E_0	$\Delta H^{0\ddagger}$	$\Delta S^{0\ddagger}$	$\log(A/s)$	E_A
$\text{C}_2\text{H}_5\text{O}^\cdot \rightarrow \cdot\text{CH}_3 + \text{CH}_2\text{O}$	71.2	72.7	13.4	14.0	75.6
$1\text{-C}_3\text{H}_7\text{O}^\cdot \rightarrow \text{CH}_3\text{CH}_2^\cdot + \text{CH}_2\text{O}$	63.4	64.7	14.8	14.1	67.6
$1\text{-C}_4\text{H}_9\text{O}^\cdot \rightarrow \text{CH}_3\text{CH}_2\text{CH}_2^\cdot + \text{CH}_2\text{O}$	58.8	60.2	16.5	14.2	63.1
$1\text{-C}_5\text{H}_{11}\text{O}^\cdot \rightarrow \text{CH}_3(\text{CH}_2)_2\text{CH}_2^\cdot + \text{CH}_2\text{O}$	57.0	58.5	17.4	14.2	61.4
$(\text{CH}_3)_2\text{CHCH}_2\text{O}^\cdot \rightarrow \text{CH}_3\text{C}^\cdot\text{HCH}_3 + \text{CH}_2\text{O}$	47.5	48.7	13.3	14.0	51.6
$(\text{CH}_3)_3\text{CCH}_2\text{O}^\cdot \rightarrow (\text{CH}_3)_3\text{C}^\cdot + \text{CH}_2\text{O}$	35.8	36.3	7.7	13.7	39.2
$2\text{-C}_3\text{H}_7\text{O}^\cdot \rightarrow \text{CH}_3^\cdot + \text{CH}_3\text{CHO}$	62.2	63.7	13.0	14.0	66.5
$2\text{-C}_4\text{H}_9\text{O}^\cdot \rightarrow \cdot\text{CH}_2\text{CH}_2 + \text{CH}_3\text{CHO}$	48.7	50.3	14.8	14.2	63.1
$2\text{-C}_5\text{H}_{11}\text{O}^\cdot \rightarrow \cdot\text{CH}_2\text{CH}_2\text{CH}_2 + \text{CH}_3\text{CHO}$	51.3	52.7	14.5	14.1	55.6
$2\text{-C}_4\text{H}_9\text{O}^\cdot \rightarrow \cdot\text{CH}_3 + \text{CH}_3\text{CH}_2\text{CHO}$	70.0	71.8	16.5	14.2	74.7
$2\text{-C}_5\text{H}_{11}\text{O}^\cdot \rightarrow \cdot\text{CH}_3 + \text{CH}_3(\text{CH}_2)_2\text{CHO}$	70.7	72.5	16.7	14.2	75.4
$t\text{-C}_4\text{H}_9\text{O}^\cdot \rightarrow \cdot\text{CH}_3 + \text{CH}_3\text{COCH}_3$	56.7	58.3	14.0	14.0	61.2
β C–C bond scission of alkoxy radicals				$\sim 14.0 \pm 0.3$	

transition state properties for the β C–C bond scission reactions of several larger alkoxy radicals. The activation entropies and enthalpies as well as the corresponding Arrhenius parameters are presented in Table 3.

For all the transition states we found the length of the breaking C–C bond significantly increased with respect to their lengths in the parent radical together with a considerably shortening of the C–O bond approaching the characteristic length of the C–O double bond. Generally, all transition state structures for the β C–C bond scission are very much product like, but this feature is less compelling with increasing the alkyl size. For smaller alkoxy radicals the transition state structures from different methods can be compared and regularly the B3LYP/SVP geometry is somewhat more product-like than the optimized MP2/6-311G(d,p) geometry. This is reflected in systematically slightly higher activation entropies from the DFT calculations. However, these differences are generally small and lead to about 10% higher A -factors. The properties of the transition states of the 12 reactions are very similar and the small geometrical differences caused a difference in the activation entropy of less than $2 \text{ J mol}^{-1} \text{ K}^{-1}$. The (O)C–C bond lengths at the transition state decrease very moderately with the increasing size of the alkyl rest, but a similar effect is seen for the equilibrium configuration of the alkoxy radical.

Since the transition state structures of the 12 reactions are very much alike, the activation entropies and Arrhenius preexponential factors are also very close (see Table 3). Consequently, we propose a unique A -factor for the β C–C bond scission of all alkoxy radicals of $A = 10^{14 \pm 0.3} \text{ s}^{-1}$. This seems to be somewhat surprising in particular when the number of methyl groups in ethoxy (1) and t -butoxy (3) decomposition are compared. The degeneracy of the three equivalent methyl groups in the t -butoxy radical cancels with the degeneracy of the three indistinguishable transition states structure of the decomposition path. This is generally true and holds also for all other cases. For the decomposition of ethoxy radicals we consequently reevaluate the Arrhenius expression and now prefer $k_\infty = 1.0 \times 10^{14} \exp(-78.2 \text{ kJ mol}^{-1}/RT) \text{ s}^{-1}$ instead of the previously published expression of $1.1 \times 10^{13} \exp(-70.3 \text{ kJ mol}^{-1}/RT) \text{ s}^{-1}$.¹¹ For i -propoxy the new Arrhenius expression of $k_\infty = 1.0 \times 10^{14} \exp(-63.1 \text{ kJ mol}^{-1}/RT) \text{ s}^{-1}$ is very similar to the recently published of $1.2 \times 10^{14} \exp(-63.7 \text{ kJ mol}^{-1}/RT) \text{ s}^{-1}$.⁹ The new activation energies are somewhat higher, however, the individual rate constants remain unchanged within the limited temperature range of the experiments.

We obtain the activation barriers for the corresponding back reactions, the addition of alkyl radicals to aldehydes, by subtracting the heat of reaction from the activation enthalpy for the decomposition direction. Using the heat of formation

of -6.0 , -45.2 and $-81.3 \text{ kJ mol}^{-1}$ for the ethoxy,¹¹ i -propoxy⁹ and t -butoxy radicals from our *ab initio* calculations we obtain reaction enthalpies of 39.2 , 20.1 and 7.4 kJ mol^{-1} , respectively. Activation barriers of 32 , 42 , and 52 kJ mol^{-1} are calculated for the addition of CH_3 radicals to CH_2O , CH_3CHO , and $(\text{CH}_3)_2\text{CO}$, respectively. Using the current literature values for the heat of formation of the alkoxy radicals^{26,27} the activation barriers would be even lower and reduce to 21 , 35 , and 42 kJ mol^{-1} , respectively. These addition reactions will compete with the currently suggested hydrogen abstraction reactions.^{4,34,35}

Conclusions

In the present study, the pressure dependence of the thermal unimolecular decomposition of the t -butoxy radical has been studied in the temperature range between 323 and 383 K . The high pressure limit has been reached at a total pressure of 60 bar helium and the falloff analysis allowed for an extrapolation of the low pressure limiting rate constant. From *ab initio* calculations we conclude that the decomposition is completely controlled by the β C–C bond scission.

A simple transition state treatment of the results of high level *ab-initio* calculations (G2(MP2) and B3LYP/SVP) provided high pressure limiting rate constants in excellent agreement with the experiment. From the results of this work and from our work on ethoxy¹¹ and i -propoxy⁹ thermal decomposition we suggest that the literature data on the thermal decomposition of all other alkoxy radicals should be critically re-evaluated. We have extensively studied the unimolecular β C–C bond scission of different alkoxy radicals using theoretical methods, based on calibrated cheap B3LYP/SVP calculations. The transition state structures were all very similar and we propose a unique preexponential factor for the β C–C bond scission of all alkoxy radical of $A = 10^{14 \pm 0.3} \text{ s}^{-1}$. The corresponding Arrhenius activation energies are generally lower than the currently accepted values in the literature. The extended study of the thermochemistry of alkoxy radicals is in progress.

Acknowledgements

We thank the Deutsche Forschungsgemeinschaft (SFB 551, "Kohlenstoff aus der Gasphase: Elementarreaktionen, Strukturen, Werkstoffe"), the Commission of European Communities (contract SARVOC) and CERLA (Centre d'Etude et Recherches Lasers et Applications) for financial support. CERLA is supported by Ministère chargé de la Recherche, Région Nord/Pas de Calais and the Fonds Européen de

Développement Economique des Régions (FEDER). B.V. thanks the Alexander von Humboldt Stiftung for a postdoctoral fellowship and the Hungarian Scientific Research Found (OTKA F030436).

Appendix

LJ-parameters:

He: $\sigma = 2.55 \times 10^{-10}$ m $\epsilon/k_B = 10$ K

t-C₄H₉O[•]: $\sigma = 5.26 \times 10^{-10}$ m $\epsilon/k_B = 402$ K

(LJ-parameters for *t*-butoxy radicals have been estimated by taking the values for alcohols. All LJ-parameters have been taken from ref. 36).

Molecular parameters calculated from the ab initio methods

Molecular frequencies were scaled by the factor 0.95:

(a) C₄H₉O

Vibrational frequencies in cm⁻¹: 165, 239, 251, 317, 319, 388, 391, 413, 730, 865, 877, 898, 923, 974, 985, 1166, 1185, 1226, 1327, 1332, 1359, 1414, 1422, 1428, 1439, 1439, 1460, 2917, 2921, 2927, 3005, 3010, 3017, 3018, 3023 and 3027

Rotational constants in cm⁻¹: 0.1653, 0.1652 and 0.1500

(b) Transition state

Vibrational frequencies in cm⁻¹: $i \times 732$, 91, 215, 228, 241, 252, 368, 459, 492, 623, 662, 752, 851, 908, 909, 1031, 1060, 1175, 1326, 1329, 1374, 1390, 1414, 1419, 1421, 1431, 1577, 2923, 2926, 2981, 3008, 3012, 3042, 3044, 3148 and 3159

Rotational constants in cm⁻¹: 0.1603, 0.1507 and 0.1374

Threshold energy: $\epsilon = 57.7$ kJ mol⁻¹

References

- A. C. Baldwin, J. R. Barker, D. M. Golden and D. G. Hendry, *J. Phys. Chem.*, 1977, **81**, 2483.
- L. Batt, *Int. Rev. Phys. Chem.*, 1987, **6**, 53.
- J. Heicklen, *J. Adv. Photochem.*, 1988, **14**, 177.
- D. L. Baulch, C. J. Cobos, R. A. Cox, C. Esser, P. Frank, Th. Just, J. A. Kerr, M. J. Pilling, J. Troe, R. W. Walker and J. Warnatz, *J. Phys. Chem. Ref. Data*, 1992, **21**, 411.
- R. Atkinson, *Int. J. Chem. Kinet.*, 1997, **29**, 99.
- L. Batt, *Int. J. Chem. Kinet.*, 1979, **11**, 977.
- L. Batt and R. T. Milne, *Int. J. Chem. Kinet.*, 1977, **9**, 549.
- M. Blitz, M. J. Pilling, S. H. Robertson and P. W. Seakins, *Phys. Chem. Chem. Phys.*, 1999, **1**, 73.
- P. Devolder, Ch. Fittschen, A. Frenzel, H. Hippler, G. Poskrebyshv, F. Striebel and B. Viskolcz, *Phys. Chem. Chem. Phys.*, 1999, **1**, 675.
- K. Hoyermann, M. Olzmann, J. Seeba and B. Viskolcz, *J. Phys. Chem.*, 1999, **103**, 5692.
- F. Caralp, P. Devolder, Ch. Fittschen, N. Gomez, H. Hippler, R. Méreau, M. T. Rayez, F. Striebel and B. Viskolcz, *Phys. Chem. Chem. Phys.*, 1999, **1**, 2935.
- T. P. W. Jungkamp, J. N. Smith and J. H. Steinfeld, *J. Phys. Chem. A*, 1997, **102**, 4392.
- G. Lendvai and B. Viskolcz, *J. Phys. Chem.*, 1998, **102**, 10777.
- T. Yamada, J. W. Bozzelli and T. Lay, *J. Phys. Chem. A*, 1999, **103**, 7646.
- T. Kortvelyesi and L. Seres, *J. Chim. Phys.*, 1996, **93**, 253.
- J. M. Park, N. W. Song and K. Y. Choo, *Bull. Korean Chem. Soc.*, 1990, **11**, 343.
- L. Batt, M. W. M. Hisham and M. Mackay, *Int. J. Chem. Kinet.*, 1989, **21**, 535.
- J. Heicklen, *Adv. Photochem.*, 1988, **14**, 177.
- J.-M. Avez, PhD Thesis, University of Lille, France, 1978.
- C. Wang, L. G. Shemesh, W. Deng, M. D. Lilien and T. S. Dibble, *J. Phys. Chem. A*, 1999, **103**, 8207.
- M. J. Frisch, G. W. Trucks, H. B. Schlegel, P. M. W. Gill, B. G. Johnson, M. A. Robb, J. R. Cheeseman, T. Keith, G. A. Petersson, J. A. Montgomery, K. Raghavachari, M. A. Al-Laham, V. G. Zakrzewski, J. V. Ortiz, J. B. Foresman, J. Cioslowski, B. B. Stefanov, A. Nanayakkara, M. Challacombe, C. Y. Peng, P. Y. Ayala, W. Chen, M. W. Wong, J. L. Andres, E. S. Replogle, R. Gomperts, R. L. Martin, D. J. Fox, J. S. Binkley, D. J. Defrees, J. Baker, J. P. Stewart, M. Head-Gordon, C. Gonzalez and J. A. Pople, Gaussian Inc., Pittsburgh PA, 1995.
- A. P. Scott and L. Radom, *J. Phys. Chem.*, 1996, **100**, 16502.
- A. D. Becke, *J. Chem. Phys.*, 1993, **101**, 5648.
- A. Schaefer, H. Horn and R. Ahlrichs, *J. Chem. Phys.*, 1992, **97**, 2571.
- N. J. Cohen, *Phys. Chem. Ref. Data*, 1996, **25**, 1411.
- J. Berkowitz, G. B. Ellison and D. Gutman, *J. Phys. Chem.*, 1994, **98**, 2744.
- D. F. McMillen and D. M. Golden, *Annu. Rev. Phys. Chem.*, 1984, **80**, 4065.
- CRC Handbook of Chemistry and Physics*, ed. D. R. Lide, CRC Press, Boca Raton, 77th edn., 1997.
- L. A. Curtiss, K. Raghavachari, G. W. Trucks and J. A. Pople, *J. Chem. Phys.*, 1991, **94**, 7221; L. A. Curtiss, K. Raghavachari, P. C. Redfern, V. Rassolov and J. A. Pople, *J. Chem. Phys.*, 1998, **109**, 7764; L. A. Curtiss, P. C. Redfern, K. Raghavachari, V. Rassolov and J. A. Pople, *J. Chem. Phys.*, 1999, **110**, 4703; A. G. Baboul, L. A. Curtiss, P. C. Redfern and K. Raghavachari, *J. Chem. Phys.*, 1999, **110**, 7650.
- J. Troe, *Ber. Bunsen-Ges. Phys. Chem.*, 1983, **87**, 161.
- R. G. Gilbert, K. Luther and J. Troe, *Ber. Bunsen-Ges. Phys. Chem.*, 1983, **87**, 169.
- J. Troe, *J. Chem. Phys.*, 1977, **66**, 4758.
- G. Z. Whitten and B. S. Rabinovitch, *J. Chem. Phys.*, 1963, **38**, 2466; G. Z. Whitten and B. S. Rabinovitch, *J. Chem. Phys.*, 1964, **41**, 1883.
- D. L. Baulch, C. J. Cobos, R. A. Cox, P. Frank, G. Hayman, Th. Just, J. A. Kerr, T. Murrells, M. J. Pilling, J. Troe, R. W. Walker and J. Warnatz, *J. Phys. Chem. Ref. Data*, 1994, **23**, 847.
- A. C. Kinsman and J. M. Roscoe, *Int. J. Chem. Kinet.*, 1994, **26**, 191.
- R. C. Reid, J. M. Prausnitz and B. E. Poling, *The Properties of Gases and Liquids*, McGraw-Hill, New York, 4th edn., 1987.

Paper b000009o